Chapter 15
Van Cittert–Zernike Theorem, Spatial Coherence, and Scattering

This chapter is concerned with the van Cittert–Zernike theorem, including an examination of the assumptions involved in its derivation, the requirement of spatial incoherence of a source, and the interferometer response to a coherent source. Some optical terminology is used, for example, *mutual coherence*, which includes complex visibility. There is also a brief discussion of some aspects of scattering by irregularities in the propagation medium. Much of the development of the theory of coherence and similar concepts of electromagnetic radiation is to be found in the literature of optics. The terminology is sometimes different from that which has evolved in radio interferometry, but many of the physical situations are similar or identical. However, in spite of the similarity, the literature shows that in the early development of radio astronomy, the optical experience was hardly ever mentioned, an exception being the reference by Bracewell (1958) to Zernike (1938) for the concept of the complex degree of coherence. The van Cittert–Zernike theorem contains a simple formalism that includes the basic principles of correlation in electromagnetic fields.

15.1 Van Cittert–Zernike Theorem

We showed in Chaps. 2 and 3 that the cross-correlation of the signals received in spaced antennas can be used to form an image of the intensity distribution of a distant cosmic source through a Fourier transform relationship. This result is a form of the van Cittert–Zernike theorem, which originated in optics. The basis for the theorem is a study published by van Cittert in 1934 and followed a few years later by a simpler derivation by Zernike. A description of the result established by van Cittert and Zernike is given by Born and Wolf (1999, Chap. 10). The original form of the result does not specifically refer to the Fourier transform relationship between intensity and mutual coherence but is essentially as follows.

A.R. Thompson, J.M. Moran, and G.W. Swenson Jr., *Interferometry and Synthesis in Radio Astronomy*, Astronomy and Astrophysics Library,
DOI 10.1007/978-3-319-44431-4_15

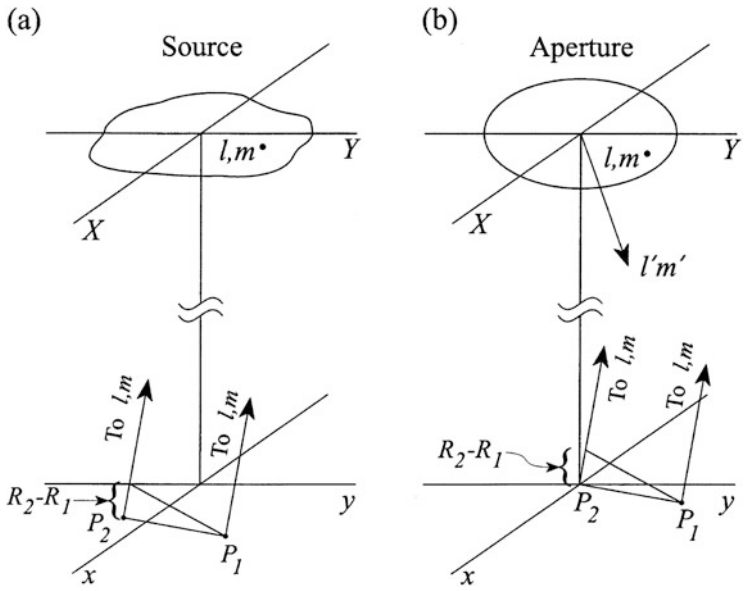

Fig. 15.1 (**a**) Geometry of a distant spatially incoherent source and the points P_1 and P_2 at which the mutual coherence of the radiation is measured. The source plane (X, Y) is parallel to the measurement plane (x, y) but at a large distance from it. (**b**) Similar geometry for measurement of the radiation field from an aperture in the (X, Y) plane that is illuminated from above by a coherent wavefront. The radiated field has a maximum at the point P_2. Direction cosines (l, m) are defined with respect to the (x, y) axes in the measurement plane, and direction cosines (l', m') are defined with respect to the (X, Y) axes in the plane of the aperture.

Consider an extended, quasi-monochromatic, incoherent source, and let the mutual coherence of the radiation be measured at two points P_1 and P_2 in a plane normal to the direction of the source, as in Fig. 15.1a. Then suppose that the source is replaced by an aperture of identical shape and size and illuminated from behind by a spatially coherent wavefront. The distribution of the electric field amplitude over the aperture is proportional to the intensity distribution over the source. The Fraunhofer diffraction pattern of the aperture is observable in the plane containing P_1 and P_2. The relative positions of the points P_1 and P_2 are the same in the two cases, but for the aperture, the geometric configuration is such that P_2 lies on the maximum of the diffraction pattern. Then the mutual coherence measured for the incoherent source, normalized to unity for zero spacing between P_1 and P_2, is equal to the complex amplitude of the field of the aperture diffraction pattern at the position P_1, normalized to the maximum value at P_2.

In this form, the theorem results from the fact that the behavior of both the mutual coherence and the Fraunhofer diffraction can be represented by similar Fourier transform relationships. Derivation of the theorem provides an opportunity

to examine the assumptions involved and is given below. The analysis is similar to that given by Born and Wolf but with some modifications to take advantage of the simplified geometry when the source is at an astronomical distance. First, we note that in optics, the *mutual coherence function* for a field $E(t)$, measured at points 1 and 2, is represented by

$$\Gamma_{12}(u, v, \tau) = \lim_{T \to \infty} \frac{1}{2T} \int_{-T}^{T} E_1(t) E_2^*(t - \tau)\, dt \,, \tag{15.1}$$

where u and v are the coordinates of the spacing between the two measurement points, expressed in units of wavelength. $\Gamma_{12}(u, v, 0)$, for zero time offset, is equivalent to the complex visibility $\mathcal{V}(u, v)$ used in the radio case.

15.1.1 Mutual Coherence of an Incoherent Source

The geometric situation for the incoherent source is shown in Fig. 15.1a. Consider the source located in a distant plane, indicated by (X, Y). The radiated field is measured at two points, P_1 and P_2, in the (x, y) plane that is parallel to the source plane. In the radio case, these points are the locations of the interferometer antennas. It is convenient to specify the position of a point in the (X, Y) plane by the direction cosines (l, m) measured with respect to the (x, y) axes. The source is sufficiently distant that the direction of any point within it measured from P_1 is the same as that measured from P_2. The fields at P_1 and P_2 resulting from a single element of the source at the point (l, m) are given by

$$E_1(l, m, t) = \mathcal{E}\left(l, m, t - \frac{R_1}{c}\right) \frac{\exp\left[-j2\pi\nu(t - R_1/c)\right]}{R_1} \,, \tag{15.2}$$

and

$$E_2(l, m, t) = \mathcal{E}\left(l, m, t - \frac{R_2}{c}\right) \frac{\exp\left[-j2\pi\nu(t - R_2/c)\right]}{R_2} \,, \tag{15.3}$$

where $\mathcal{E}(l, m, t)$ is a phasor representation of the complex amplitude of the electric field at the source for an element at position (l, m). R_1 and R_2 are the distances from this element to P_1 and P_2, respectively, and c is the velocity of light. The exponential terms in Eqs. (15.2) and (15.3) represent the phase change in traversing the paths from the source to P_1 and P_2.

The complex cross-correlation of the field voltages at P_1 and P_2 due to the radiation from the element at (l, m) is, for zero time offset,

$$\begin{aligned}\Big\langle E_1(l,m,t)\ E_2^*(l,m,t)\Big\rangle &= \left\langle \mathcal{E}\left(l,m,t-\frac{R_1}{c}\right)\ \mathcal{E}^*\left(l,m,t-\frac{R_2}{c}\right)\right\rangle \\ &\quad\times \frac{\exp[-j2\pi\nu(t-R_1/c)]\exp[j2\pi\nu(t-R_2/c)]}{R_1R_2} \\ &= \left\langle \mathcal{E}(l,m,t)\ \mathcal{E}^*\left(l,m,t-\frac{R_2-R_1}{c}\right)\right\rangle \frac{\exp\left[j2\pi\nu(R_1-R_2)/c\right]}{R_1R_2}\ ,\end{aligned} \tag{15.4}$$

where the superscript asterisk denotes the complex conjugate, and the angle brackets $\langle\ \rangle$ represent a time average. Note that the source is assumed to be spatially incoherent, which means that terms of the form $\langle E_1(l_p, m_p, t)E_2^*(l_q, m_q, t)\rangle$, where p and q denote different elements of the source, are zero. If the quantity $(R_2 - R_1)/c$ is small compared with the reciprocal receiver bandwidth, we can neglect it within the angle brackets of Eq. (15.4), where it occurs in the amplitude term for $\mathcal{E}$. Equation (15.4) then becomes

$$\langle E_1(l,m,t)\ E_2^*(l,m,t)\rangle = \frac{\langle \mathcal{E}(l,m,t)\mathcal{E}^*(l,m,t)\rangle \exp\left[j2\pi\nu(R_1-R_2)/c\right]}{R_1R_2}\ . \tag{15.5}$$

The quantity $\langle \mathcal{E}(l,m,t)\ \ \mathcal{E}^*(l,m,t)\rangle$ is a measure of the time-averaged intensity, $I(l, m)$, of the source. To obtain the mutual coherence function of the fields at points P_1 and P_2, we integrate over the source, using ds to represent an element of area within the (X, Y) plane:

$$\Gamma_{12}(u,v,0) = \int_{\text{source}} \frac{I(l,m)\exp\left[j2\pi\nu(R_1-R_2)/c\right]}{R_1R_2}\,ds\ , \tag{15.6}$$

where u and v are the x and y components of the spacing between the points P_1 and P_2 measured in wavelengths. Note that $(R_1 - R_2)$ is the differential distance in the path lengths from (l, m) in the source to P_1 and P_2. The points P_1 and P_2 have coordinates (x_1, y_1) and (x_2, y_2) respectively, so $u = (x_1 - x_2)\nu/c$ and $v = (y_1 - y_2)\nu/c$, where c/ν is the wavelength. Thus, we obtain $(R_2 - R_1) = (ul + vm)c/\nu$. Because the distance of the source is very much greater than the distance between P_1 and P_2, for the remaining R terms, we can put $R_1 \simeq R_2 \simeq R$, where R is the distance between the (X, Y) and (x, y) origins. Then $ds = R^2 dl\, dm$, and from Eq. (15.6),

$$\Gamma_{12}(u,v,0) = \int\int_{\text{source}} I(l,m)\, e^{-j2\pi(ul+vm)}\,dl\,dm\ . \tag{15.7}$$

Since the integrand in Eq. (15.7) is zero outside the source boundary, the limits of the integral effectively extend to infinity, and the mutual coherence $\Gamma_{12}(u, v, 0)$, which is equivalent to the complex visibility $\mathcal{V}(u, v)$, is the Fourier transform of the intensity distribution $I(l, m)$ of the source. This result is generally referred to as the van Cittert–Zernike theorem. However, it is instructive to examine the definition of the theorem in terms of the diffraction pattern of an aperture, given at the beginning of this section.

15.1.2 *Diffraction at an Aperture and the Response of an Antenna*

The Fraunhofer diffraction field of an aperture, as a function of angle, can be analyzed using the geometry shown in Fig. 15.1b. Here, an aperture is illuminated by an electromagnetic field of amplitude $\mathcal{E}(l, m, t)$, where again we use direction cosines with respect to the x and y axes to indicate points within the aperture as seen from P_1 and P_2. The (x, y) plane is in the far field of a wavefront from any point in the aperture, so such a wavefront can be considered plane over the distance P_1P_2. The aperture is centered on the (X, Y) origin and is normal to the line from the (X, Y) origin to P_2. The phase over the aperture is assumed to be uniform, and components of the field therefore combine in phase at P_2. Thus, in the (x, y) plane, the maximum field strength occurs at P_2. Now consider the field at the point P_1, which has coordinates (x, y). The component of the field at P_1 due to radiation from an element of the aperture at position (l, m) is given by Eq. (15.2). The path lengths from the point (l, m) at the source to P_1 and P_2 are R_1 and R_2, respectively, and $R_2 - R_1 = lx + my$. Thus, from Eq. (15.2), we can write

$$E_1(l, m, t) = \frac{e^{-j2\pi\nu(t-R_2/c)}}{R_1}\,\mathcal{E}\left(l, m, t - \frac{R_1}{c}\right) e^{-j2\pi\nu(xl+ym)/c}\,. \tag{15.8}$$

Again, for the remaining R terms, we put $R_1 \simeq R_2 \simeq R$. Integration over the aperture then gives the total field at P_1,

$$E(x, y) = \frac{e^{-j2\pi\nu(t-R/c)}}{R}\int_{\text{aperture}} \mathcal{E}\left(l, m, t - \frac{R}{c}\right) e^{-j2\pi[(x/\lambda)l+(y/\lambda)m]}ds\,, \tag{15.9}$$

where λ is the wavelength, and the element of area ds is proportional to $dl\,dm$. The term on the right side that is outside the integral is a propagation factor that represents the variation in amplitude and phase over the path from the source to P_2 in Fig. 15.1b. In applying the result to the radiation pattern of an aperture, we replace the time-dependent functions E and $\mathcal{E}$ by the corresponding rms field amplitudes,

which will be denoted by $\overline{E}$ and $\overline{\mathcal{E}}$, respectively:

$$\overline{E}(x,y) \propto \int\int_{\text{aperture}} \overline{\mathcal{E}}(l,m)\, e^{-j2\pi[(x/\lambda)l+(y/\lambda)m]} dl\, dm\ , \tag{15.10}$$

where the propagation factor in Eq. (15.9) has been omitted. A comparison of Eqs. (15.7) and (15.10) explains the van Cittert–Zernike theorem as described at the beginning of this section. With the specified proportionality between the incoherent intensity and the coherent field amplitude, it will be found that

$$\frac{\Gamma_{12}(u,v,0)}{\Gamma_{12}(0,0,0)} = \frac{\overline{E}(x,y)}{\overline{E}(0,0)}\ . \tag{15.11}$$

In Eqs. (15.7) and (15.10), the integrand is zero outside the source or aperture. Thus, in each case, the limits of integration can be extended to $\pm\infty$, and the equations are seen to be Fourier transforms. The calculations of the mutual coherence of the source and the radiation pattern of the aperture yield similar results because the geometry and the mathematical approximations are the same in each case. It should be emphasized, however, that the physical situations are different. In the first case considered, the source is spatially incoherent over its surface, whereas in the second case, the field across the aperture is fully coherent.

The result in Eq. (15.10) also gives the angular radiation pattern for an antenna that has the form of an excited aperture. The application to an antenna is more useful if the radiation pattern is specified in terms of an angular representation (l', m') of the direction of radiation from the antenna aperture instead of the position of the point P_1, and if the field distribution over the aperture is specified in terms of units of length rather than angle. (l', m') are direction cosines with respect to the (X, Y) axes. Since the angles concerned are small, we can substitute into Eq. (15.10) $x = Rl'$, $y = Rm'$, $l = X/R$, $m = Y/R$, $dl = dX/R$, and $dm = dY/R$, and obtain

$$\overline{E}'(l', m') \propto \int\int_{\text{aperture}} \overline{\mathcal{E}}_{XY}(X,Y) e^{-j2\pi[(X/\lambda)l'+(Y/\lambda)m']}\, dX\, dY\ . \tag{15.12}$$

This is the expression for the field distribution resulting from Fraunhofer diffraction at an aperture [see, e.g., Silver (1949)]. It includes the case of a transmitting antenna in which the aperture of a parabolic reflector is illuminated by a radiator at the focus. If such an antenna is used in reception, the received voltage from a source in direction (l', m') is proportional to the right side of Eq. (15.12). Thus, the voltage reception pattern $V_A(l', m')$, introduced in Sect. 3.3.1, is proportional to the right side of Eq. (15.12).

To obtain the power radiation pattern for an antenna, we need the response in terms of $|\overline{E}'(l', m')|^2$. From an autocorrelation theorem of Fourier transforms, the squared amplitude of $\overline{E}'(l', m')$ is equal to the autocorrelation of the Fourier transform of $\overline{E}'(l', m')$ [see, e.g., Bracewell (2000), and note that this relationship

is also a generalization of the Wiener–Khinchin relationship derived in Sect. 3.2]. Thus, the power radiated as a function of angle is given by

$$|\overline{E}'(l',m')|^2 \propto \int\int_{\text{aperture}} [\overline{\mathcal{E}}_{XY}(X,Y) \star\star \overline{\mathcal{E}}_{XY}(X,Y)] e^{-j2\pi[(X/\lambda)l'+(Y/\lambda)m']}\, dX\, dY \ , \tag{15.13}$$

where $\overline{\mathcal{E}}(X,Y) \star\star \overline{\mathcal{E}}(X,Y)$ is the two-dimensional autocorrelation function of the field distribution over the aperture. To obtain absolute values of the radiated field, the required constant of proportionality can be determined by integrating Eq. (15.13) over 4π steradians to obtain the total radiated power and equating this to the power applied to the antenna terminals. In reception, the power collected by an antenna is proportional to the power radiated in transmission, so the form of the beam is identical in the two cases. To illustrate the physical interpretation of Eq. (15.13), consider the simple case of a rectangular aperture with uniform excitation of the electric field. The function $\overline{\mathcal{E}}_{XY}(X,Y)$ is then the product of two one-dimensional functions of X and Y. If d is the aperture width in the X direction, the autocorrelation function in X is triangular with a width $2d$, and Fourier transformation gives

$$|\overline{E}_X(l')|^2 \propto \left[\frac{\sin(\pi d l'/\lambda)}{\pi d l'/\lambda}\right]^2 . \tag{15.14}$$

In the l' dimension, the full width of this beam at the half-power level is $0.886\lambda/d$, for example, 1° for $d/\lambda = 50.8$ wavelengths. For a uniformly illuminated circular aperture of diameter d, the response pattern is circularly symmetrical and is given by

$$|\overline{E}_r(l'_r)|^2 \propto \left[\frac{2J_1(\pi d l'_r/\lambda)}{\pi d l'_r/\lambda}\right]^2 , \tag{15.15}$$

where the subscript r indicates a radial profile in which l'_r is measured from the center of the beam, and J_1 is the first-order Bessel function. The full width of the beam at the half-power level is $\sim 1.03\lambda/d$.

A more direct way of obtaining the Fraunhofer radiation pattern of an aperture antenna is to start by considering the field strength of the radiated wavefront as a function of direction, rather than the field strength at a single point P_1, as above. However, the method used was chosen to provide a more direct comparison with the interferometer response to a spatially incoherent source. For a more detailed analysis of the response of an antenna, see, for example, Booker and Clemmow (1950), Bracewell (1962), or the textbooks on antennas in the Further Reading of Chapter 5.

15.1.3 Assumptions in the Derivation and Application of the van Cittert–Zernike Theorem

At this point, it is convenient to collect and review the assumptions and limitations that are involved in the theory of the interferometer response.

1. *Polarization of the electric field.* Although the electric fields are vector quantities with directions that depend on the polarization of the radiation, the components received by antennas from different elements of the source can be combined in the manner of scalar quantities. The fields are measured by antennas at P_1 and P_2, and each antenna responds to the component of the radiation for which the polarization matches that of the antenna. If the fields are randomly polarized and the antennas are identically polarized, then the signal product in Eq. (15.4) represents half the total power at each antenna. However, the antenna polarizations do not have to be identical since, in general, the interferometer system will respond to some combination of components of the source intensity determined by the antenna polarizations. The ways in which the antenna polarizations can be chosen to examine all polarizations of the incident radiation are described in Sect. 4.7.2. Thus, the scalar treatment of the field involves no loss of generality.
2. *Spatial incoherence of the source.* The radiation from any point on the source is statistically independent from that from any other point. This applies almost universally to astronomical sources and permits the integration in Eq. (15.6) by allowing cross products representing different elements of the source to be omitted. The Fourier transform relationship provided by the van Cittert–Zernike theorem requires the source to be spatially incoherent. Spatial coherence and incoherence are discussed in Sect. 15.2. Note that an incoherent source gives rise to a coherent or partially coherent wavefront as its radiation propagates through space. If this were not the case, the mutual coherence (or visibility) of an incoherent source, measured by spaced antennas, would always be zero.
3. *Bandwidth pattern.* The assumption required in going from Eqs. (15.4) to (15.5), that $(R_2 - R_1)/c$ is less than the reciprocal bandwidth $(\Delta\nu)^{-1}$, can be written

$$\frac{\Delta\nu}{\nu} < \frac{1}{l_d u}\,, \qquad \frac{\Delta\nu}{\nu} < \frac{1}{m_d v}\,, \tag{15.16}$$

   where l_d and m_d are the maximum angular dimensions of the source. This is the requirement that the source be within the limits imposed by the bandwidth pattern of the interferometer, which is discussed in Sect. 2.2. Conversely, the required field of view limits the maximum bandwidth that can be used in a single receiving channel. The distortion caused by the bandwidth effect is discussed further in Sect. 6.3.1 and, if not severe, can often be corrected.
4. *Distance of the source.* For an array with maximum baseline D, the departure of the wavefront from a plane, for a source of distance R, is $\sim D^2/R$. Thus, the *far-field* distance R_{ff}, defined as that for which the divergence is small compared

with the wavelength λ, is given by

$$R_{ff} \gg D^2/\lambda \ . \tag{15.17}$$

The far-field condition implies that the antenna spacing subtends a small angle as seen from the source and results in the approximation for Fraunhofer diffraction. If the source is at a known distance closer than the far-field distance, then the phase term can be compensated. This may sometimes be necessary in solar system studies. For example, for an antenna spacing of 35 km and a wavelength of 1 cm, the far-field distance is greater than 1.2×10^{11} m, or approximately the distance to the Sun. On the other hand, the distances to sources in the near field such as Earth-orbiting satellites can be determined from measurements of the wavefront curvature (e.g., Sect. 9.11). When the source is in the far-field distance, no information concerning its structure in the line-of-sight direction is possible, only the intensity distribution as projected onto the celestial sphere. (Line-of-sight structure can be determined by modeling velocity structure.)

5. *Use of direction cosines.* In going from Eqs. (15.6) to (15.7), the path difference $(R_2 - R_1)$ is specified in terms of the baseline coordinates (u, v) and angular coordinates (l, m). The expression for the path difference is precise if l and m are specified as direction cosines. In integration over the source, the element of area bounded by increments $dl\,dm$ is equal to $dl\,dm/n$, where n is the third direction cosine and is equal to $\sqrt{1 - l^2 - m^2}$. In optics, derivation of the van Cittert–Zernike theorem usually involves the assumption that the source subtends only small angles at the measurement plane. Then l and m can be approximated by the corresponding small angles, and n can be approximated by unity. As a result, the relationship between $\mathcal{V}$ and I becomes a two-dimensional Fourier transform, as in the approximation for limited field size discussed in Sect. 3.1.1. In the radio case, the less restrictive result in Eq. (3.7) is sometimes required.
6. *Three-dimensional distribution of the visibility measurements.* As antennas track a source, the antenna-spacing vectors, designated above by (u, v) components, may not lie in a plane, and three coordinates, (u, v, w), are then required to specify them. The Fourier transform relationship is then more complicated, but a simplifying approximation can be made if the field of view to be imaged is small. These effects are discussed in Sect. 11.7.
7. *Refraction in space.* It has been implicitly assumed in the analysis above that the space between the source and the antennas is empty, or at least that any medium within it has a uniform refractive index, so that there is no distortion of the incoming wavefront from the source. However, the interstellar and interplanetary media, and the Earth's atmosphere and ionosphere, can introduce effects including rotation of the position angle of a linearly polarized component, as discussed in Chaps. 13 and 14.

15.2 Spatial Coherence

In the derivation of the interferometer response in Chaps. 2 and 3, and in Eq. (15.5), it is assumed that the source under discussion is spatially incoherent. This means that the waveforms received from different spatial elements of the source are not correlated, which enables us to add the correlator output from the different angular increments in the integration over the source. We now examine this requirement in more detail. To illustrate the principles involved, it is sufficient to work in one dimension on the sky, for which the position is given by the direction cosine l.

15.2.1 Incident Field

Consider the electric field $E(l,t)$ at the Earth's surface resulting from a wavefront incident from the direction l at time t. Figure 15.2 shows the geometry of the situation, in which $l = 0$ in the direction OS of the center, or nominal position, of the source under observation. l is a direction cosine measured from OB, the normal to OS. A path OS' is shown that indicates the direction of another part of the source. Radiation from the direction OS' produces a wavefront parallel to OB'. The wavefronts from points on the source are plane because we are considering a source in the far field of the interferometer. The line OA represents the projection of the baseline normal to the direction of the source, and the distance OA measured in wavelengths is equal to u. Now consider wavefronts from the directions S and S' that arrive at the same time at O. To reach the point A, the wavefront from S' has to travel a farther distance AA'. With the usual small-angle approximation, we find that the distance AA' is equal to ulc/ν, that is, ul wavelengths. Thus, the wave from direction S' is delayed at A by a time interval $\tau = ul/\nu$, relative to the wave from S. If we represent the wave from direction S' by $E(l,t)$ at O, at A it is $E(l, t-\tau)$.

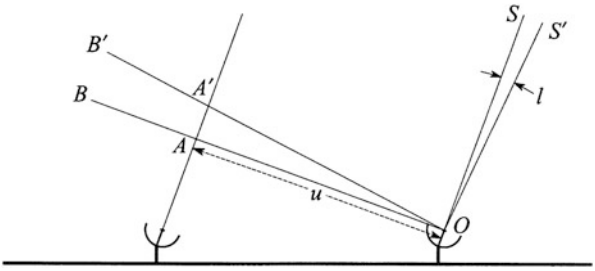

Fig. 15.2 Diagram to illustrate the variation of phase along a line OB that is perpendicular to the direction of a source OS, where l is the direction cosine that specifies the direction OS' and is defined with respect to OB. The angle SOS' is small and is thus approximately equal to l, as indicated. The line OS' points toward another part of the same source, and OB' is perpendicular to it.

Now because the incident wavefronts are plane, the amplitude of the wave does not change over the distance AA'. However, the phase changes by $\nu\tau = ul$, so for the wave from S' at A, we have

$$E(l, t-\tau) = E(l, t)\, e^{-j2\pi ul} . \tag{15.18}$$

If $e(u, t)$ is the field at A resulting from radiation from all parts of the source, then

$$e(u, t) = \int_{-\infty}^{\infty} E(l, t)\, e^{-j2\pi ul} dl . \tag{15.19}$$

It will be assumed that the angular dimensions of the source are not large, so also we have

$$E(l, t) = 0, \qquad |l| \geq 1 . \tag{15.20}$$

The condition specified in Eq. (15.20) allows us to write the limits of the integral in Eq. (15.19) as $\pm\infty$. Note that Eq. (15.19) has the form of a Fourier transform, and the inverse transform gives $E(l, t)$ from $e(u, t)$. Equation (15.19) will be required in the following subsection.

15.2.2 Source Coherence

We now return to the spatial coherence of the source and follow part of a more extensive analysis by Swenson and Mathur (1968). As a measure of the spatial coherence, we introduce the *source coherence function* γ. This is defined in terms of the cross-correlation of signals received from two different directions, l_1 and l_2, at two different times:

$$\begin{aligned} \gamma(l_1, l_2, \tau) &= \lim_{T\to\infty} \frac{1}{2T} \int_{-T}^{T} E(l_1, t) E^*(l_2, t-\tau)\, dt \\ &= \langle E(l_1, t) E^*(l_2, t-\tau) \rangle . \end{aligned} \tag{15.21}$$

Finite limits are used in the integral to ensure convergence. $\gamma(l_1, l_2, \tau)$ is similar to the coherence function of a source or object discussed by Drane and Parrent (1962) and Beran and Parrent (1964).

The *complex degree of coherence* of an extended source is the normalized source coherence function

$$\gamma_N(l_1, l_2, \tau) = \frac{\gamma(l_1, l_2, \tau)}{\sqrt{\gamma(l_1, 0)\gamma(l_2, 0)}} , \tag{15.22}$$

where $\gamma(l_1, \tau)$ is defined by putting $l_1 = l_2$ in Eq. (15.21), that is, $\gamma(l_1, \tau) = \gamma(l_1, l_2, \tau)$. It can be shown by using the Schwarz inequality that $0 \leq |\gamma_N(l_1, l_2, \tau)| \leq 1$. The extreme values of 0 and 1 correspond to the cases of complete incoherence and complete coherence, respectively. When dealing with extended sources of arbitrary spectral width, it is possible that, for a given pair of points l_1 and l_2, $|\gamma_N(l_1, l_2, \tau)|$ is zero for one value of τ and nonzero for another value. Therefore, more stringent definitions of complete coherence and incoherence are necessary. The following definitions are adapted from Parrent (1959):

1. The emissions from the directions l_1 and l_2 are completely coherent (incoherent) if $|\gamma_N(l_1, l_2, \tau)| = 1$ (0) for all values of τ.
2. An extended source is coherent (incoherent) if the emissions from all pairs of directions l_1, l_2 within the source are coherent (incoherent).

In all other cases, the extended source is described as partially coherent.

Consider now the coherence function of the field $e(x_\lambda, t)$ of a distant source measured, say, at the Earth's surface, x_λ being a linear coordinate measured in wavelengths in a direction normal to $l = 0$:

$$\begin{aligned}\Gamma(x_{\lambda 1}, x_{\lambda 2}, \tau) &= \lim_{T\to\infty} \frac{1}{2T} \int_{-T}^{T} e(x_{\lambda 1}, t) e^*(x_{\lambda 2}, t-\tau)\, dt \\ &= \langle e(x_{\lambda 1}, t) e^*(x_{\lambda 2}, t-\tau) \rangle \ . \end{aligned} \tag{15.23}$$

This is a variation of the mutual coherence function Γ_{12} in Eq. (15.1), in which the positions of the measurement points defined by $x_{\lambda 1}$ and $x_{\lambda 2}$ are retained, rather than just the relative positions given by the baseline components. By using the Fourier transform relationship between $E(l, t)$ and $e(u, t)$ derived in Eq. (15.19), and replacing u by x_λ, we obtain

$$\Gamma(x_{\lambda 1}, x_{\lambda 2}, \tau) = \int_{-\infty}^{\infty} \int_{-\infty}^{\infty} \gamma(l_1, l_2, \tau) e^{-j2\pi(x_{\lambda 1} l_1 - x_{\lambda 2} l_2)} dl_1\, dl_2 \ , \tag{15.24}$$

and the inverse transform, which is

$$\gamma(l_1, l_2, \tau) = \int_{-\infty}^{\infty} \int_{-\infty}^{\infty} \Gamma(x_{\lambda 1}, x_{\lambda 2}, \tau)\, e^{j2\pi(x_{\lambda 1} l_1 - x_{\lambda 2} l_2)} dx_{\lambda 1}\, dx_{\lambda 2} \ . \tag{15.25}$$

The relationships in Eqs. (15.24) and (15.25) do not provide a means of measuring the intensity distribution of a source, except in the case of complete incoherence. For complete incoherence, the coherence function can be expressed as

$$\gamma(l_1, l_2, \tau) = \gamma(l_1, \tau)\, \delta(l_1 - l_2) \ , \tag{15.26}$$

where δ is the delta function. Using the relation in Eq. (15.26) in conjunction with Eqs. (15.24) and (15.25), we find that the self-coherence function of a completely

incoherent source and its spatial frequency spectrum are Fourier transforms of each other:

$$\Gamma(u,\tau) = \int_{-\infty}^{\infty} \gamma(l,\tau)\, e^{-j2\pi ul} dl \tag{15.27}$$

$$\gamma(l,\tau) = \int_{-\infty}^{\infty} \Gamma(u,\tau)\, e^{j2\pi ul} du\ , \tag{15.28}$$

where $u = x_{\lambda 1} - x_{\lambda 2}$. It is clear that $\Gamma(u,\tau)$ is independent of $x_{\lambda 1}$ and $x_{\lambda 2}$ and depends only on their difference. Thus, u can be interpreted as the spacing of two sample points between which the coherence of the field is measured, and also as the spatial frequency of the visibility measured over the same baseline. For $\tau = 0$, from Eqs. (15.21) and (15.26), we obtain

$$\gamma(l,0) = \left\langle |E(l)|^2 \right\rangle\ , \tag{15.29}$$

which is the one-dimensional intensity distribution of the source, I_1, introduced in Eq. (1.10). Then from Eqs. (15.27) and (15.29),

$$\Gamma(u,0) = \int_{-\infty}^{\infty} \left\langle |E(l)|^2 \right\rangle e^{-j2\pi ul} dl\ . \tag{15.30}$$

$\Gamma(u,0)$ is measured between points along a line normal to the direction $l = 0$. As measured with an interferometer, it is also the complex visibility $\mathcal{V}$. Eq. (15.30) is the Fourier transform relationship between mutual coherence (visibility) and intensity.

When the incoherence condition in Eq. (15.26) is introduced into Eqs. (15.24) and (15.25), two results appear: the van Cittert–Zernike relation between mutual coherence and intensity, and the stationarity of the mutual coherence with respect to u. The physical reason underlying these results is seen in Fig. 15.2. When the wavefronts incident at different angles combine at any point, the relative phases of their (Fourier) frequency components vary linearly with the position of the point (e.g., the position of A along the line OB in Fig. 15.2), and for small l, they also vary linearly with the angle on the sky. As a result, the phase differences of the Fourier components at two points depend only on the relative positions of the points, not their absolute positions. Interferometer measurements of mutual coherence incorporate the phase differences for a range of angles of incidence governed by the angular dimensions of the source and the width of the antenna beams. The linear relationship between phase and position angle allows us to recover the angular distribution of the incident wave intensity from the variation of the mutual coherence as a function of u, by Fourier analysis. If the angular width of the source is small enough that the distance AA' in Fig. 15.2 is always much less than the wavelength, then the form of the electric field remains constant along the line OA, and the source is not resolved.

15.2.3 Completely Coherent Source

Parrent (1959) has shown that an extended source can be completely coherent only if it is monochromatic. As examples of such a source, one may visualize the aperture of a distant, large antenna, or an ensemble of radiating elements all driven by the same monochromatic signal. The aperture considered in Sect. 15.1.2 is a conceptual example of a coherent source. The difference between the responses of an interferometer to a fully coherent source and to a fully incoherent one can be explained by the following physical picture. The source can be envisioned as an ensemble of radiators distributed over a solid angle on the sky. In the case of a coherent source, the signals from the radiators are monochromatic and coherent. The radiation in any direction combines into a single monochromatic wavefront and produces a monochromatic signal in each antenna of an interferometer. The output of the correlator is directly proportional to the product of the two (complex) signal amplitudes from the antennas. Thus, if a coherent source is observed with n_a antennas, the $n_a(n_a - 1)/2$ pairwise cross-correlations of the signals that are measured can be factored into n_a values of complex signal amplitude.

In contrast, for an incoherent source, the outputs from radiating elements are uncorrelated and must be considered independently. Each one produces a component of the fringe pattern in the correlator output. But since the phases of these fringe components depend on the positions of the radiators within the source, the combined response is proportional not only to the signal amplitudes at the antennas but also to a factor that depends on the angular distribution of the radiators. This factor, of magnitude ≤ 1, is equal to the modulus of the visibility normalized to unity for an unresolved (point) source of flux density equal to that of the source under observation. Unless the source is unresolved, it is not possible to factor the measured cross-correlations into signal amplitude values at the antennas. Because the emissions of the radiating elements of a source are uncorrelated, the information on the source distribution is preserved in the ensemble of wavefronts they produce at the antennas.

As shown by the derivation of the angular dependence of the radiation from a coherently illuminated aperture [Eq. (15.12)], and suggested by the analogy with a large antenna, the radiation from a coherent source is highly directional. Thus, the signal strengths observed depend on the absolute positions of the two antennas of an interferometer, as in Eqs. (15.24) and (15.25), not only on their relative positions, as is the case for an incoherent source. The ability to factor the signal outputs from a series of baselines, and the nonstationarity of the correlator output measurements with the absolute positions of the antennas, are two characteristics that could allow a coherent source to be recognized (MacPhie 1964). From the analysis in Sect. 15.1, it is clear that a similar range of antenna spacings is required to resolve an incoherent source or to explore the radiation pattern of a coherent source of the same angular size.

15.3 Scattering and the Propagation of Coherence

It is well known that optical telescope images of single stars made with exposure times short compared with the timescale of atmospheric scintillation exhibit multiple stellar images (see Sect. 17.6.4). These images result from the scattering of light from the star by irregularities in the Earth's atmosphere. Something closely analogous to this occurs in the case of imaging of an unresolved radio source through a medium with strong irregular scattering, such as the interplanetary medium within a few degrees of the Sun, as described in Sect. 14.3. Since each scattered image results from the emission of the same source, one is led to expect that such a situation would simulate the effect of a distribution of coherent point sources. In this section, we examine the effects of scattering by considering the propagation of coherence in space, following in part a discussion by Cornwell et al. (1989). This formalism suggests methods for the recovery of the unscattered image from the observed image.

Given a radiating surface, we wish to know the mutual coherence function on another (possibly virtual) surface in space. In the typical radio astronomy situation, a number of simplifying assumptions can be made about the geometry of the problem. Consider the situation illustrated in Fig. 15.3, in which narrowband radio waves propagate from surface S to surface Q. The mutual coherence of two points in space is the expectation of the product of the (copolarized) electric fields at the two points.

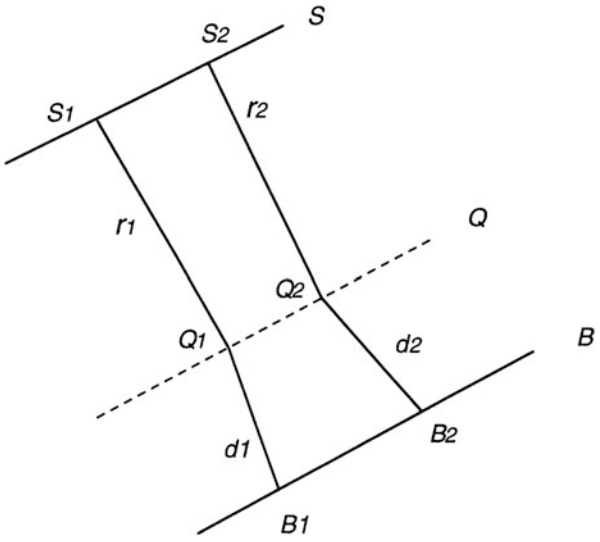

Fig. 15.3 Simplified geometry for examining the propagation of coherence. S represents an extended source, Q is the location of a scattering screen, and B is the measurement plane. Surfaces S, Q, and B are plane and parallel, and r_1, r_2, d_1, and d_2 are much greater than the wavelength. All rays are nearly (but not necessarily exactly) perpendicular to the surfaces.

For signals correlated with arbitrary time delay, the mutual coherence is

$$\Gamma(Q_1, Q_2, \tau) = \langle E(Q_1, t) E^*(Q_2, t-\tau) \rangle \ . \tag{15.31}$$

The mutual coherence function Γ is a function of the field at two points and the time difference τ. We consider the propagation of *mutual intensity*, that is, the mutual coherence evaluated for $\tau = 0$. Following common practice, we represent the mutual intensity by $J(Q_1, Q_2) \equiv \Gamma(Q_1, Q_2, 0)$. J will be subscripted by S, Q, or B to indicate the corresponding plane (Fig. 15.3) of the mutual intensity value. We assume that the emitting surface is completely incoherent, as is usually the case for astronomical objects, and that the observed radiation is restricted to a narrow band of frequencies, as dictated by the characteristics of the receiving system. From Eq. (15.31) and the Huygens–Fresnel formulation of radiation, it can be shown (Born and Wolf 1999, Goodman 1985), by a calculation similar to the one used in deriving Eq. (15.6), that the mutual intensity for points Q_1 and Q_2 is

$$J_Q(Q_1, Q_2) = \lambda^{-2} \int \int_S J_S(S_1, S_2) \frac{\exp[-j2\pi(r_1 - r_2)/\lambda]}{r_1 \, r_2} \, dS_1 \, dS_2 \ , \tag{15.32}$$

where $dS_1 \, dS_2$ is a surface element of S, and λ is the wavelength at the center of the observed frequency band.

The condition of incoherence can be represented by the use of a delta function (Beran and Parrent 1964), as in Eq. (15.26). Here, the mutual intensity is represented by a delta function, and thus, the intensity distribution on the surface Q is found by allowing points Q_1 and Q_2 to merge:

$$J_S(S_1, S_2) = \lambda^2 I(S_1) \, \delta(S_1 - S_2) \ , \tag{15.33}$$

where the factor λ^2 has been included to preserve the physical dimension of intensity. Equation (15.32) then becomes

$$J_Q(Q_1, Q_2) = \int_S I(S_1) \frac{\exp[-j2\pi(r_1 - r_2)/\lambda]}{r_1 \, r_2} \, dS \ . \tag{15.34}$$

When the angular dimension of the source is infinitesimal, that is, when the source is unresolved, the integration over the source becomes trivial, and the mutual intensity can be factored into terms depending, respectively, on r_1 and r_2:

$$J_Q(Q_1, Q_2) = I(S) \left(\frac{\exp(-j2\pi r_1/\lambda)}{r_1} \right) \left(\frac{\exp(j2\pi r_2/\lambda)}{r_2} \right) \ , \tag{15.35}$$

where r_1 and r_2 now originate at a single point S. In the more general case of a resolved source, Eq. (15.34) cannot be factored. Equations (15.34) and (15.35) describe for their respective cases the propagation of mutual coherence in situations subject to the constraints of Fig. 15.3 and thus can be used to determine the

mutual intensity on surface Q resulting from incoherent radiation from surface S. Examination of Eq. (15.31) reveals that, for the extended source S, the mutual intensity on Q depends on both r_1 and r_2 for all pairs of points on Q. Thus, the field at Q is at least partially coherent for all sources, including those of finite extent. This is intuitively reasonable, as all points on Q are illuminated by all points on S. In fact, it can be demonstrated rigorously that an incoherent field cannot exist in free space (Parrent 1959).

Suppose now that we have a situation in which the surface Q is actually a screen of irregularities in the transmission medium, such as plasma or dust, which scatters the radiation from S. The mutual intensity incident on the screen is modified by a complex transmission factor $T(Q)$ to produce the transmitted mutual intensity

$$J_{Qt}(Q_1, Q_2) = T(Q_1)T^*(Q_2)J_{Qi}(Q_1, Q_2) \, , \tag{15.36}$$

where subscripts i and t indicate the incident and transmitted mutual intensity, respectively. From Eq. (15.34), we now define a "propagator" (Cornwell et al. 1989) for mutual intensity:

$$W(S, B) = \int_S \frac{T(Q) \exp[-j2\pi(r + d)/\lambda]}{r\, d} \, dS \, , \tag{15.37}$$

where r and d are defined in Fig. 15.3. Then the mutual intensity on surface B is given, in terms of the mutual intensity of an extended source S, by

$$J_B(B_1, B_2) = \lambda^{-4} \int \int_S J_S(S_1, S_2) W(S_1, B_1) W^*(S_2, B_2) \, dS_1 \, dS_2 \, . \tag{15.38}$$

For an incoherent extended source,

$$J_B(B_1, B_2) = \lambda^{-2} \int_S I(S) W(S, B_1) W^*(S, B_2) \, dS \, , \tag{15.39}$$

and for a point source of flux density F, the mutual intensity on B becomes

$$J_B(B_1, B_2) = F\lambda^{-2} W(S, B_1) W^*(S, B_2) \, . \tag{15.40}$$

Again, for the unresolved source, the mutual intensity on B consists of two factors, each depending only on one position on B. However, for an extended incoherent source distribution on S, the mutual intensity depends on *differences* in position and therefore cannot be factored.

The existence of a scattering screen between a source and an observer, with an instrument of limited aperture, raises the possibility of greatly increased angular resolution resulting from the much larger extent of the scattering screen. The partial coherence of radiation from the screen requires that the intensity be measured at all points on the measurement plane B, spaced as dictated by the Nyquist

criterion, rather than at all points in the spatial frequency spectrum as allowed by the van Cittert–Zernike theorem. The former observing mode results in very much more data than does the latter. In two spatial dimensions, a large redundancy of data results, so that in principle, not only can the scattering screen be characterized, but the source as well. In this respect, the problem is similar to that of self-calibration (Sect. 11.3.2). Unfortunately, in the case of the scattering screen, the practical difficulties of such observations are enormous, and few significant attempts have been made to apply the principle. Cornwell and Narayan (1993) discuss the possibilities of statistical image synthesis using scattering to obtain ultrafine resolution in a manner somewhat analogous to speckle imaging (see Sect. 17.6.4).

Emission from a radio source that undergoes strong scattering during propagation through space has been investigated by Anantharamaiah et al. (1989), and Cornwell et al. (1989). To demonstrate the response of a radio telescope to such a spatially coherent source distribution, they observed the strong and essentially pointlike source 3C279, which passes close to the Sun each year. Under these conditions, the scattering is strong enough to cause amplitude scintillation of the received signals. Anantharamaiah and colleagues used the VLA in its most extended configuration, for which the longest baselines are approximately 35 km. The velocity of the solar wind, of order 100–400 km s^{-1}, causes irregularities to sweep across the array in $\sim$100 ms, so it was necessary to make snapshot observations of duration 10–40 ms to avoid smearing of the image by the movement of the scattering screen. Observations were made at wavelengths of 20, 6, and 2 cm, with the source at angular distances of 0.9° to 5° from the Sun. It was found that the correlator output values could be factored as expected for a coherent source. When correlated signals were averaged for about 6 s, an enlarged image of the source was obtained, and the enlargement increased as the distance from the Sun decreased. It was also demonstrated that it would be possible to determine the characteristics of the scattering screen by measuring the mutual intensity function on the ground, provided that the latter is measured completely in the two-dimensional spatial frequency domain. It is not possible to distinguish between a spatially coherent extended source and a scattering screen illuminated by a point source.

A significant observation was made by Wolszczan and Cordes (1987), who were able to infer the dimensions of structure within pulsar PSR 1237+25 from an occurrence of interstellar scattering. The pulsar was observed with a single antenna, the 308-m-diameter spherical reflector at Arecibo, at a frequency of 430 MHz. Dynamic spectra of the received signal (i.e., the received power displayed as a function of both time and frequency) showed prominent band structure with maxima separated by $\sim$ 300–700 kHz in frequency. This was interpreted in terms of a thin-screen model of the interstellar medium, in which refraction of rays from the pulsar occurred at two separated points in the screen. The analysis of such a model is complicated by the occurrence of both diffractive and refractive scattering, resulting from structure smaller and larger than the Fresnel scale, respectively (Cordes et al. 1986). The refraction gave rise to two images of the source at the radio telescope, resulting in fringes in the intensity of the received signal. The distance of the pulsar (0.33 kpc) and its transverse velocity (178 km s^{-1}) were

known from other observations, and the distance of the screen was taken to be half the distance of the pulsar. It was deduced that the angular separation of the images was $\sim$ 3.3 mas, corresponding to a spacing of $\sim$1 AU (astronomical unit) between the refracting structures. In effect, the refracting structures constitute a two-element interferometer, with fringe spacing $\sim$ 1 μas. For comparison, the angular resolution of a baseline equal to the diameter of the Earth at 430 MHz would be 44 mas. The particular conditions that resulted in this observation lasted for at least 19 days, and during that period, observations of other pulsars did not show similar scattering. This strongly suggests that the observed phenomenon resulted from a fortuitous configuration of the interstellar medium in the direction of the pulsar.

Apart from cases of scattering such as that described, there are essentially no clear cases of spatially coherent astronomical sources, although coherent mechanisms may occur in pulsars and masers (Verschuur and Kellermann 1988). Fully coherent sources are not amenable to synthesis imaging using the van Cittert–Zernike principle and thus do not fall within the area of principal concern of this book. Further material on coherence and partial coherence can be found, for example, in Beran and Parrent (1964), Born and Wolf (1999), Drane and Parrent (1962), Mandel and Wolf (1965, 1995), MacPhie (1964), and Goodman (1985).

References

Anantharamaiah, K.R., Cornwell, T.J., and Narayan, R., Synthesis Imaging of Spatially Coherent Objects, in *Synthesis Imaging in Radio Astronomy*, Perley, R.A., Schwab, F.R., and Bridle, A.H., Eds., Astron. Soc. Pacific Conf. Ser., **6**, 415–430 (1989)

Beran, M.J., and Parrent Jr., G.B., *Theory of Partial Coherence*, Prentice-Hall, Englewood Cliffs, NJ, 1964; repr. by Society of Photo-Optical Instrumentation Engineers, Bellingham, WA (1974)

Booker, H.G., and Clemmow, P.C., The Concept of an Angular Spectrum of Plane Waves, and Its Relation to That of Polar Diagram and Aperture Distribution, *Proc. IEE*, **97**, 11–17 (1950)

Born, M., and Wolf, E., *Principles of Optics*, 7th ed., Cambridge Univ. Press, Cambridge, UK (1999)

Bracewell R.N., Radio Interferometry of Discrete Sources, *Proc. IEEE*, **46**, 97–105 (1958)

Bracewell, R.N., Radio Astronomy Techniques, in *Handbuch der Physik*, Vol. 54, Flugge, S., Ed., Springer-Verlag, Berlin (1962), pp. 42–129.

Bracewell, R.N., *The Fourier Transform and Its Applications*, McGraw-Hill, New York, 2000 (earlier eds. 1965, 1978)

Cordes, J.M., Pidwerbetsky, A., and Lovelace, R.V.E., Refractive and Diffractive Scattering in the Interstellar Medium, *Astrophys. J.*, **310**, 737–767 (1986)

Cornwell, T.J., Anantharamaiah, K.R., and Narayan, R., Propagation of Coherence in Scattering: An Experiment Using Interplanetary Scintillation, *J. Opt. Soc. Am.*, **6A**, 977–986 (1989)

Cornwell, T.J., and Narayan, R., Imaging with Ultra-Resolution in the Presence of Strong Scattering, *Astrophys. J. Lett.*, **408**, L69–L72 (1993)

Drane, C.J., and Parrent Jr., G.B., On the Mapping of Extended Sources with Nonlinear Correlation Antennas, *IRE Trans. Antennas Propag.*, **AP-10**, 126–130 (1962)

Goodman, J.W., *Statistical Optics*, Wiley, New York (1985)

MacPhie, R.H., On the Mapping by a Cross Correlation Antenna System of Partially Coherent Radio Sources, *IEEE Trans. Antennas Propag.*, **AP-12**, 118–124 (1964)

Mandel, L., and Wolf, E., Coherence Properties of Optical Fields, *Rev. Mod. Phys.*, **37**, 231–287 (1965)

Mandel, L., and Wolf, E., *Optical Coherence and Quantum Optics*, Cambridge Univ. Press, Cambridge, UK (1995)

Parrent, Jr. G.B., Studies in the Theory of Partial Coherence, *Opt. Acta*, **6**, 285–296 (1959)

Silver, S., *Microwave Antenna Theory and Design*, Radiation Laboratory Series, Vol. 12, McGraw-Hill, New York (1949), p. 174

Swenson, Jr. G.W., and Mathur, N.C., The Interferometer in Radio Astronomy, *Proc. IEEE*, **56**, 2114–2130 (1968)

Verschuur, G.L., and Kellermann, K.I., Eds., *Galactic and Extragalactic Astronomy*, Springer-Verlag, New York (1988)

Wolszczan, A., and Cordes, J.M., Interstellar Interferometry of the Pulsar PSR 1237+25, *Astrophys. J. Lett.*, **320**, L35–L39 (1987)

Zernike, F., Concept of Degree of Coherence and Its Application to Optical Problems, *Physica*, **5**, 785–795 (1938)